Structural and regulatory diversity shape HLA-C protein expression levels

Gurman Kaur[1], Stephanie Gras[2,3], Jesse I. Mobbs[2,3], Julian P. Vivian[2,3], Adrian Cortes[4,5], Thomas Barber[4], Subita Balaram Kuttikkatte[1], Lise Torp Jensen[6], Kathrine E. Attfield[1], Calliope A. Dendrou[4], Mary Carrington[7,8], Gil McVean[5], Anthony W. Purcell[2], Jamie Rossjohn[2,3,9*], Lars Fugger[1,4,6*]

[1]MRC Human Immunology Unit, Weatherall Institute of Molecular Medicine, John Radcliffe Hospital, University of Oxford, Oxford, OX3 9DS, UK.

[2]Infection and Immunity Program and the Department of Biochemistry and Molecular Biology, Biomedicine Discovery Institute, Monash University, Clayton, Victoria 3800, Australia.

[3]Australian Research Council Centre of Excellence in Advanced Molecular Imaging, Monash University, Clayton, Victoria 3800, Australia.

[4]Oxford Centre for Neuroinflammation, Nuffield Department of Clinical Neurosciences, Division of Clinical Neurology, John Radcliffe Hospital, University of Oxford, Oxford, OX3 9DS, UK.

[5]Wellcome Trust Centre for Human Genetics, University of Oxford, Oxford, OX3 7BN, UK.

[6]Department of Clinical Medicine, Aarhus University Hospital, 8200 N Aarhus, Denmark.

[7]Cancer and Inflammation Program, Leidos Biomedical Research Inc., Frederick National Laboratory for Cancer Research, Frederick, MD 21702, USA.

[8]The Ragon Institute of MGH, MIT and Harvard, Cambridge, MA 02139, USA.

[9]Institute of Infection and Immunity, Cardiff University, School of Medicine, Heath Park, Cardiff, CF14 4XN, UK.

*Correspondence: lars.fugger@imm.ox.ac.uk or jamie.rossjohn@monash.edu

ABSTRACT

Expression of HLA-C varies widely across individuals in an allele-specific manner. This variation in expression can influence efficacy of the immune response, as shown for infectious and autoimmune diseases. MicroRNA binding partially influences differential HLA-C expression, but the additional contributing factors have remained undetermined. Here we demonstrate using functional and structural analyses that HLA-C expression is modulated not just at the RNA level but also at the protein level. Specifically, we show that variation in exons 2 and 3, which encode the α1/α2 domains, drives differential expression of HLA-C allomorphs at the cell surface by influencing the structure of the peptide-binding cleft and the diversity of peptides bound by the HLA-C molecules. Together with our phylogenetic analyses, these results highlight the diversity and long-term balancing selection of regulatory factors that modulate HLA-C expression.

The human leukocyte antigen *(HLA)* gene locus is one of the most diverse regions of the human genome, with extreme polymorphism and associations with a large number of human diseases[1]. HLA molecules have diverse clinical implications in infectious and autoimmune diseases, cancer, transplantation, and in pregnancy[2,3]. While antigenic specificity is important in dictating the immune response driven by

the HLA molecule, HLA protein levels at the cell surface also play an important role in controlling the strength of the immune response[4,5]. Indeed, cytokine-driven up-regulation of cell surface HLA in an acute infection highlights the importance of HLA expression levels in mediating host defence against pathogens[6].

HLA class I molecules, encoded by *HLA-A*, *HLA-B* and *HLA-C*, are highly polymorphic and can bind and present a range of intracellular peptides to cytotoxic CD8+ T cells, as well as regulate innate immune responses by interacting with killer cell immunoglobulin-like receptors (KIR) expressed on natural killer (NK) cells[2,3]. While much is known regarding the role of HLA-A and HLA-B molecules in protective and aberrant immunity, comparatively little is known about HLA-C. Compared to its counterparts, HLA-C is expressed at lower cell surface levels, is less polymorphic, and has evolved to have more extensive interactions with KIRs, thereby playing a key role in regulating NK cell responses[7-10].

HLA-C expression varies widely in an allele-specific manner[4,11] and this diversity is an important determinant in influencing disease outcome, especially as observed in the case of HIV-1 infection[4,12-14]. Thus, high HLA-C protein expression in the host has been associated with protection against the HIV-1 virus, increased cytotoxic T lymphocyte responses and increased frequency of viral escape mutations, suggesting that higher HLA-C expression exerts a selection pressure on the virus[4], which is in line with the recently discovered virus-mediated down-regulation of HLA-C expression[15]. In contrast, high HLA-C expression levels correlate with increased risk of Crohn's disease[4,11], and in cases of unrelated hematopoietic transplantation, with

poor outcome and graft-versus-host disease[5]. The divergent effects of HLA-C expression on infectious and autoimmune diseases, combined with evidence for the recent origin of mutations that influence expression[16], suggest a dynamic evolutionary balance between positive and negative gene regulation, which can shift with the epidemiological cycling of specific pathogens.

There has been a wide interest in identifying factors that influence differential expression of HLA-C molecules. A single nucleotide polymorphism 35 kb upstream of *HLA-C* (-35 C/T) was correlated with HIV-1 viral load and HLA-C expression in people of European ancestry[12,14,17]. However, it was subsequently shown that this variant was not causative, and was in linkage disequilibrium with another variant in the 3' untranslated region (UTR) of *HLA-C*, which is a polymorphic microRNA binding site for miR-148a. *HLA-C* alleles that have an intact miR-148a binding site, such as *C*07* and *C*03* amongst others, have low expression as a result of inhibition by the microRNA, whereas other *HLA-C* alleles (e.g. *C*05*, *C*08*) that escape miR-148a binding due to a deletion in the miR binding site, are expressed at higher levels. This insertion/deletion polymorphism in the 3'UTR of *HLA-C* is only fractionally responsible for the differential surface expression of *HLA-C* alleles[13]. Variation in miR-148a expression itself has also been shown to further influence HLA-C levels. However, this still does not fully account for the variation in expression of HLA-C alleles with an intact miR-148a binding site, and has no impact on those alleles that escape miR-148a regulation[11]. Alleles of HLA-C show a continuous rather than a bimodal expression pattern, suggesting that additional factors with stronger effects

than the miR binding site are primarily responsible for influencing differential HLA-C surface expression[13].

To further understand the mechanisms responsible for differential HLA-C expression, we chose two *HLA-C* alleles, *C*05* and *C*07*, which are commonly found at allele frequencies ranging between 3-14% (C*05) and 18-38% (C*07) in Caucasian populations[18], have high and low expression, respectively, and differ in the 3'UTR miR-148a binding site variant. Using a series of functional and structural analyses, we show that variation in exons 2 and 3, which encode the antigen-binding α1 and α2 domains of HLA-C molecules, contributes to differential cell surface expression of these *HLA-C* allomorphs. This regulation is found to be post-transcriptional as the differential cell surface expression does not correlate with mRNA levels. Furthermore, we observe that HLA-C*07 has a deeper and narrower antigen-binding cleft than the relatively flat peptide-binding cleft of HLA-C*05. In line with this, HLA-C*05 binds a larger range of peptides than HLA-C*07, which can stabilise it on the cell surface, hence offering a potential explanation for the differential cell surface expression of these *HLA-C* allomorphs.

RESULTS

Differential expression of *HLA-C* alleles

To investigate the mechanisms responsible for differential expression of *HLA-C* molecules, we selected two common *HLA-C* alleles, *HLA-C*05:01:01:01* (referred to as *C*05*) and *HLA-C*07:02:01:03* (referred to as *C*07*), that differ in expression levels, and have either a disrupted (*C*05*) or intact (*C*07*) miR-148a binding site,

respectively. To study the involvement of the different parts of the *HLA-C* gene in contributing towards differential surface expression, we generated hybrid *C*05* and *C*07* genomic constructs. One half of these hybrid constructs, consisting of the promoter, 5'UTR, exons 1-3 and introns 1, 2 and part of intron 3, was taken from the human *HLA-C*05* or *HLA-C*07* alleles, whilst the second half of the constructs were identical, and consisted of part of intron 3, exons and introns 4-8, and the 3'UTR of the murine *H-2K*^{b} allele (Fig. 1a); this allowed us to exclude the involvement of the miR-148a binding in differential HLA-C expression levels. Importantly, similar hybrid constructs for other HLA class I genes have been described before, and shown to retain the peptide-binding specificity of the HLA allele[19]. The *C*05* and *C*07* hybrid constructs were transfected into HLA class I-negative 721.221 cells along with a GFP plasmid to control for transfection efficiency, and the level of HLA-C surface expression on transfected cells was determined by flow cytometry. We observed a ~2-fold higher expression of HLA-C*05 on the cell surface of transfected cells, in comparison to cells that expressed HLA-C*07 (Fig. 1b,c and Supplementary Fig. 1a). This relative expression difference between *C*05* and *C*07* transfected cells was physiologically relevant as it was comparable to the relative difference in expression between HLA-C*05 and HLA-C*07 on human peripheral blood lymphocytes, which is reported to be between 1.5 and 2-fold[4]. This was of particular interest considering that both our hybrid constructs had an identical 3'UTR, as well as a region starting from a part of intron 3 until, and including, exon 8. These findings therefore indicated that variations either in the promoter, 5'UTR, exons 1-3 (which includes the peptide-binding cleft) or introns 1-3, of *HLA-C*05* and *HLA-C*07* were contributing to the differential HLA-C expression.

Influence of the promoter/5'UTR of *HLA-C* on gene expression

To test whether the promoter/5'UTRs of the *HLA-C*05* and *HLA-C*07* alleles were driving the protein-level differences that we observed, we cloned their promoter/5'UTR sequences (including a region 776 or 766 bp prior to the start codon respectively) upstream of the luciferase gene in a promoter-less vector (Fig. 2a). HEK 293T cells and 721.221 cells were transfected with these C*05-luciferase and C*07-luciferase constructs and relative luciferase activity was measured. Surprisingly, the promoter/5'UTR of *C*07* led to a significantly (~2-fold) higher expression of the luciferase reporter gene in comparison to the *C*05* promoter (Fig. 2b,c) - an effect which was in the opposite direction of what was observed on the cell surface of *C*05*- and *C*07*-transfected cells. This differential effect of the promoter/5'UTR of *C*07* on luciferase expression has been evidenced in a previous study, that included the region of its core promoter, and reported that the core promoter of *C*07* was significantly more active than its *C*06* counterpart[20]. To assess how the promoter directly influenced expression of the HLA-C molecules, we swapped the promoter/5'UTR of *C*05* and *C*07*, and generated new hybrid constructs (Fig. 2d), which were transfected into 721.221 cells. Swapping of the promoters did not result in a change in cell surface expression of C*05 and C*07: C*05 was consistently expressed at higher levels (~2-fold relative to C*07) on the cell surface, irrespective of the promoter/5'UTR driving its transcription (Fig. 2e,f and Supplementary Fig. 1b). Thus, despite having a seemingly weaker promoter/5'UTR region, the cell surface protein levels of HLA-C*05 remained significantly higher as compared to HLA-C*07. As the variation in the promoter/5'UTR of these alleles could not explain their

differential protein expression, this inferred that the relevant region was between exons and introns 1-3.

Variation in exons 2 and 3 affects differential HLA-C expression

To specifically investigate if the exonic coding region of *HLA-C* could have a direct effect on HLA-C expression levels, we used a lentiviral expression system, where the expression of the coding region of *C*05* and *C*07* was driven by a common lentiviral promoter. Although the anti-HLA antibody (W6/32) that we used to stain for HLA-C expression has monomorphic specificity and binds fully assembled HLA class I molecules with equal affinity[21,22], we included an N-terminal hemagglutinin (HA) tag in these constructs as an additional control. To establish the validity of the system, HA-tagged *C*05* and *C*07* constructs including the sequence of exons 1-8 of these alleles were generated (Fig. 3a), and 721.221 cells were transduced with the respective C*05 and C*07 lentivirus at equivalent multiplicity of infection (normalised using GFP, expressed in tandem from the lentiviral expression vector). The differential expression pattern of HLA-C, detected on the cell surface by the anti-HLA (Fig. 3b,d), and anti-HA (Fig. 3c,e) antibodies, was preserved in these lentiviral-transduced cells at levels similar to those observed with the transiently transfected cells (Fig. 1c and Fig. 2f). Importantly, the expression difference between C*05 and C*07 was seen to be consistent between HA-tagged and non-tagged *HLA-C* constructs, suggesting that the HA tag, itself, does not change the HLA-C expression pattern or cellular characteristics, also shown by a previous study comparing HA-tagged and non-tagged HLA class I molecules[23]. To then test whether variation in α1 and α2 domains of the HLA-C molecules was responsible for the differential

expression, we generated modified lentiviral expression constructs that contained only exons 1-3 of the *C*05* and *C*07* alleles and exons 4-8 of the murine *H-2K^b* allele (Fig. 4a). Interestingly, cell surface staining revealed a significant and consistently high expression (~1.7-fold) of C*05 in comparison to C*07 in 721.221 cells transduced with the modified lentivirus, demonstrating that variation in the α1/α2 domains of HLA-C was controlling the differential HLA-C expression (Fig. 4b-e). Furthermore, this appeared to be a post-transcriptional event, as no significant changes in HLA-C were observed at the mRNA level, as tested using exon-spanning QPCR primers designed for an *H-2K^b* region common to both *HLA-C* constructs (Supplementary Fig. 2). Additionally, staining for HLA-C after fixation and permeabilisation of transduced cells (Supplementary Fig. 3 and Supplementary Fig. 4), or quantification of HLA-C protein levels by immunoblotting of whole cell lysates (Supplementary Fig. 5 and Supplementary Fig. 6), did not reveal a difference in total protein-level expression between C*05 and C*07, despite the cell-surface difference (Fig. 3 and 4). This may be related to accumulation and retention of HLA-C folding intermediates inside the cell, prior to successful peptide loading and export to the cell surface, such that total protein expression is unaffected but there is a differential expression level at the plasma membrane[24,25]. Taken together, these data demonstrate that variation in the coding region of HLA-C, specifically the α1 and α2 domains, can drive differential HLA-C expression at the cell surface.

HLA-C*05 and HLA-C*07 possess contrasting antigen-binding clefts

To elucidate the role of α1/α2 domains and the peptide-binding cleft of HLA-C on differential expression, we solved the structure of HLA-C*05 in complex with a HLA-

C*05 specific peptide, SAEPVPLQL (SAE)[26], and HLA-C*07 in complex with a HLA-C*07 specific peptide, RYRPGTVAL (RYR)[27] (Supplementary Table 1).

Within the HLA-C*05-SAE complex, there are four main anchor residues, P1-Ser, P3-Glu, P7-Leu and P9-Leu. The P1-Ser is surrounded by seven aromatic residues, arising from the floor of the antigen-binding cleft (Tyr7, Tyr67 and Phe33) and from the α1 and α2 helices (Tyr59, Tyr171, Tyr159 and Trp167), as well as hydrogen bonding to Lys66 (Fig. 5a). The P3-Glu forms a salt bridge with Arg156 and Arg97, and has a hydrophobic interaction with Tyr159 (Fig. 5b). In addition, the P7-Leu places its hydrophobic side chain underneath Arg156 and binds within a hydrophobic pocket lined by Phe116 and Trp147 (Fig. 5c). Finally, the P9-Leu is anchored in the F pocket of HLA-C*05 and interacts with the 2 hydrophobic residues, Leu81 and Leu95 (Fig. 5d).

The structure of HLA-C*07 in complex with the RYR peptide revealed canonical P2-Tyr and P9-Leu anchor residues, a large network of interactions at P1-Arg and a secondary anchor residue at P3-Arg. The P1-Arg in HLA-C*07 was stabilised by aromatic residues, similarly to the P1-Ser of the SAE peptide in HLA-C*05 (not shown), with an additional salt bridge formed with the Glu63 (Fig. 5e). The large P2-Tyr sat into the B pocket, stabilised by hydrogen bond with Asp9 and van der Waals interactions with Tyr7 and Tyr67 (Fig. 5e). In contrast to HLA-C*05, the B pocket of HLA-C*07 is deeper due to the smaller polymorphic residue at position 9, which is Asp in HLA-C*07, as opposed to Tyr in HLA-C*05. The P3-Arg of the RYR peptide, which was buried within the antigen-binding cleft, acted as a secondary anchor residue when binding to the HLA-C*07 molecule. The absence of the Arg156 in HLA-C*07 (replaced with a smaller and hydrophobic Leu156) allowed the P3-Arg of the

RYR peptide to fit inside the cleft of the HLA-C*07 molecule (Fig. 5f). The buried conformation of the P3-Arg is facilitated by the presence of small residues at position 9 (Asp→Tyr) and 99 (Ser→Tyr) in the cleft of HLA-C*07 that allow enough space for the Arg97 to move away from the P3-Arg (Fig. 5f). P3-Arg is stabilised by a hydrogen bond with the Gln70 and salt bridge with Asp114. The P9-Leu interacts with the HLA-C*07 in a similar fashion to the analogous interaction observed for HLA-C*05-SAE complex (not shown).

HLA-C*05 and HLA-C*07 differ by 22 residues, of which 15 are located within the α1/α2 domains, with 10 of these being involved in peptide interactions, namely Tyr9, Thr73, Asn77, Lys80, Tyr99, Asn114, Phe116, Trp147, Glu152 and Arg156 (Fig. 5g). While HLA-C*05 uses a large network of aromatic residues in both the A and B pockets, the HLA-C*07 B pocket lacks two of these tyrosines (Tyr9 → Asp9 and Tyr99 → Ser99) (Fig. 6a). The presence of these smaller residues and Asp9 in HLA-C*07 is consistent with the preference of P2 Arg/Tyr for HLA-C*07-restricted peptides, as previously reported[28]. Similarly, the F pocket of HLA-C*05 was 'filled' by large aromatic residues (Phe116 and Trp147), which were absent from HLA-C*07 (Ser116 and Leu147) (Fig. 6b). In addition to the larger Trp147, the hinge of the α2-helix of HLA-C*05 differs from HLA-C*07 by two other large residues, namely Glu152 (Ala152 in HLA-C*07) and Arg156 (Leu156 in HLA-C*07). These large residues located on the α2-helix of HLA-C*05 open the antigen-binding cleft by almost 3Å (residues 149 to 151) (Fig. 6c), while the rest of the cleft was similar (r.m.s.d. of 0.62 Å on the Cα of the α1-α2 domains).

Overall the B and F pockets, binding the characteristic anchor residues at P2 and the C-terminus of HLA class I-restricted epitopes, contain large aromatic residues in HLA-C*05 that are absent in HLA-C*07. Consequently, the antigen-binding cleft of HLA-C*05 is composed of residues with large side chains, and accordingly offers a more shallow cleft (volume 1200 $Å^3$, Fig. 6d) in contrast to the HLA-C*07 cleft that is deeper and narrower with a larger volume (1500 $Å^3$, Fig. 6e). Therefore, the polymorphic residues are 'filling' the cleft of HLA-C*05 that represents a relatively shallow groove, providing a 'peptide-landing platform' for HLA-C*05, instead of the traditional groove generally found in HLA molecules that are more prone to have preference for specific anchoring motifs (Fig. 6d,e).

The apparent 'flat cleft' of HLA-C*05 might allow binding of a more diverse range of peptides, which could impact the stability of the peptide-HLA-C complexes and contribute to differential HLA-C expression at the cell surface. To test this, we refolded both HLA-C*05 and HLA-C*07 with four different peptides, including two HLA-C*05 peptides (a self-peptide, ITASRFKEL (ITA)[29], and the viral peptide SAE[26] and two HLA-C*07 peptides (two self peptides, RYRPGTVAL (RYR)[27] and KYFDEHYEY (KYF)[30]), and compared the thermal stability of these peptide-HLA-C complexes. In line with the structural data, HLA-C*07 showed a preference for P2 Arg/Tyr, and its stability was 5-10°C higher when refolded with the HLA-C*07 peptides, RYR and KYF, in comparison to its stability with the HLA-C*05 peptides, SAE and ITA. Contrastingly, the HLA-C*05 molecule exhibited the same thermal stability with the HLA-C*05 peptides as well as the HLA-C*07 peptides, with an average Tm of ~52°C (Supplementary Table 2). In line with the structural analyses,

these results indicate that, unlike for HLA-C*07, the stability of HLA-C*05 was less reliant on the sequence of the bound peptides, and that HLA-C*05 might be more permissive than HLA-C*07 in its peptide-binding motif, which could impact its differential expression pattern.

Comparison of the peptides bound by HLA-C*05 and HLA-C*07

To compare the peptide repertoire of HLA-C*05:01 and HLA-C*07:02, we isolated these HLA class I molecules from the cell surface of equal numbers of *C*05* and *C*07* transfected 721.221 cells, and sequenced bound peptides by mass spectrometry.

A total of 1870 specific peptides were identified from HLA-C*05 molecules (Supplementary Data File 1). The majority of these peptides (70.6 %) were 8-10 amino acids in length, with nonamers being the most abundant species (46.7 %) (Fig. 7a). Analysis of nonameric peptides revealed three positions with conserved residues (P2, P3 and P9). The P3 position was by far the most conserved with 80 % of the peptides having an Asp at this position, and a further 15 % having Glu. The P2 position optimally preferred a small uncharged residue such as Ala (40 %), and to a smaller extent Ser (13 %) and Val (11 %). At the P9 position, the majority of the peptides carried a hydrophobic residue, with 45 % of the peptides carrying a Leu, with smaller contributions from Phe (17 %), Met (13 %) and Val (10%) (Fig. 7c).

A total of 580 specific peptides were identified from HLA-C*07 molecules (Supplementary Data File 1). The majority of the peptides observed (54.1 %) were also 8-10 amino acids in length, with nonamers being the most abundant species (39.8%), however, this was less than that observed for HLA-C*05 (Fig. 7b). Analysis

of nonamers revealed only two positions with conserved residues (P2 and P9). The P2 position was most conserved with Arg being most dominant (40 %), closely followed by Tyr (38 %), and a small contribution from Lys (13 %). The P9 position preferred a hydrophobic residue with Leu (31 %) being most conserved, however HLA-C*07 also appeared to accept larger hydrophobic residues such as Tyr (30 %), Phe (17 %) and Met (13 %) (Fig. 7d).

In line with the structural analysis, these peptide-repertoire data demonstrate that the number of distinct peptides bound by HLA-C*05 were 3-fold higher than those bound by HLA-C*07, in agreement with the higher relative expression of HLA-C*05 on the cell surface. Collectively, these data provide insight into how the α1/α2 domains and the peptide-binding cleft of HLA-C molecules can not only have a direct influence on HLA stability and peptide repertoire, but also influence cell surface expression levels.

Phylogenetic analysis of *HLA-C* sequences

To assess the evolutionary origin of the variation in exons 2 and 3 of *HLA-C* alleles, which we show influences HLA-C expression levels, we performed sequence alignments of the exon 2 and 3 region of *HLA-C* alleles with the available non-human primate *MHC-C* alleles, and inferred their phylogenetic relationship (Fig. 8). Within the exon 2 and 3 sequence, the *HLA-C*07* alleles seemed more closely related to a set of chimpanzee *Patr-C* alleles, than to *HLA-C*05* alleles. This indicated a maintenance of *HLA-C*07*-like alleles in non-human primates, whereas the *HLA-C*05*-like alleles have only been found in humans. As expected, there was also evidence for additional diversity, and groups of chimpanzee-specific *MHC-C* and human-specific *HLA-C* sequences.

Our study, combined with previous work[13], suggests that there are three regions of *HLA-C* that have the ability to regulate differential HLA-C expression i.e. the promoter/5'UTR, exons 2 and 3, and the 3'UTR. To compare the diversity of genetic variants in these three regions, we performed phylogenetic analysis for each of these regions across a range of *HLA-C* alleles (Supplementary Fig. 7). These phylogenetic trees were then used to calculate phylogenetic distances between *HLA-C* alleles for each of these regions. Using *HLA-C*05* and *HLA-C*07* as references, the degree of similarity between a *HLA-C* allele and *HLA-C*05* or *HLA-C*07* was determined for each region, and plotted as a grid (Fig. 9). This *in silico* analysis revealed a wide range of variation in the three genetic regions that regulate HLA-C expression, which could be related to the observed continuous expression pattern of *HLA-C* alleles. For example, *C*04* alleles, which have been shown to be expressed at high levels at the cell surface[4], appear to be more similar to *C*05* than to *C*07* in the promoter/5'UTR, and exon 2 and 3 sequence. This is particularly interesting for C*04, as, based on binding of miR-148a in the 3'UTR of its mRNA[13], and its similarity to *C*07* in the 3'UTR, it would have been predicted to be a low-expresser (Fig. 9). These patterns of genetic diversity suggest that a combination of variants spread throughout the *HLA-C* gene region, and perhaps additional factors, all contribute towards allele-specific differential expression of HLA-C at both the transcript and protein levels.

DISCUSSION

In this study, we sought to understand the mechanisms that contribute to differential expression of HLA-C molecules. By using a comparison between two common *HLA-*

C alleles, *HLA-C*05* and *HLA-C*07*, we demonstrate that variation in exons 2 and 3 of *HLA-C*, that encode for the peptide-binding α1/α2 domains, contributes to differential cell surface HLA-C protein expression. While HLA-C*05 and HLA-C*07 levels remain unchanged at the transcript and total protein level, we find a significant difference in their relative cell surface expression, with HLA-C*05 being expressed at high levels on the cell surface. Using structural, thermal stability and peptide-repertoire comparisons, we demonstrate that the peptide-binding cleft of HLA-C*05 is more permissive and is filled with large aromatic residues, which is not the case for HLA-C*07. Our data demonstrate that instead of forming a groove as in HLA-C*07, the peptide-binding cleft of HLA-C*05 forms a flatter 'peptide-landing platform', that allows binding of a larger range of peptides, which can stabilise the HLA-C molecule, in turn affecting its expression levels on the cell surface.

We found that the promoter/5'UTR of *HLA-C*, which, in this study, spanned up to 776/766 bases upstream of the start codon, did not directly impact the differential surface expression of HLA-C alleles. This was surprising considering that the same promoter/5'UTR region differentially affected the expression of the luciferase reporter gene. A previous study suggested that an enhancer κB element in the core *HLA-C* promoter was responsible for its differential effect on the luciferase reporter, however, they did not investigate the direct effects of the core promoter on HLA-C expression levels[20]. We do not find any evidence that the region of the promoter/5'UTR of HLA-C tested in this study has any significant effect on *HLA-C* mRNA levels, however, it is feasible that elements outside of the tested sequence could impact mRNA expression of *HLA-C* alleles.

Studies on HLA molecules have largely focussed on their peptide binding specificities, whilst there has been limited emphasis on the regulatory mechanisms that control their differential allele expression and the ensuing functional implications. Small differences in expression level of *MHC/HLA* genes can influence response to pathogens, tumours, autoimmunity, as well as transplantation, potentially through both the acquired and innate immune response pathways[4,5,11,31-34]. Hence, even a two-fold difference that is observed between HLA-C allotypes, such as HLA-C*05 and HLA-C*07, is likely to have functional consequences in influencing the efficacy of the immune response. HLA-C is expressed at lower levels and is limited in polymorphism compared to its counterparts, HLA-A and HLA-B[7-10]. However, HLA-C is a prototypical KIR ligand and is important in the regulation of NK cell activity[7]. Although KIRs are capable of binding multiple HLA-C allotypes, it is plausible that differences in expression of HLA-C allotypes have a downstream influence on KIR signalling and NK cell function. The broad peptide specificity of KIRs[35] raises the question of whether alleles such as *HLA-C*05*, whose stability is less reliant on the sequence of the bound peptide, are potentially better KIR ligands.

A previous study that attempted to understand the peptide-binding specificities of HLA-C molecules suggested that no conservation at P2 is observed for HLA-C*05-restricted peptides, hence allowing a greater diversity of amino acids to bind the B pocket[28]. However, the authors described that a HLA-C*05-specific peptide would have a preference for an Asp at position 3. Our structure of the HLA-C*05-SAE complex showed that P3-Glu forms a salt bridge with the polymorphic residue Arg156

(Leu156 in HLA-C*07), and a P3-Asp would be suited to interact in the same fashion. Furthermore, results from our thermal stability assay show that smaller residues, such as P3-Ala, could also be readily accommodated within HLA-C*05. Our peptide-elution data demonstrate that HLA-C*05 has a preference for a small residue at P2, which fits well with its shallow and flat peptide-binding cleft, and its ability to bind a greater number and range of peptides.

Post-transcriptional mechanisms such as inefficient peptide binding or association with chaperons such as TAP (transporter associated with peptide-loading) or tapasin have been proposed to contribute towards lower surface expression of HLA-C in comparison to HLA-A and HLA-B[24,25,36], however, this has not yet been reported for differential surface expression of *HLA-C* alleles.

Studies of chicken MHC have reported an inverse correlation between diversity of peptide repertoire and cell surface MHC class I expression, with low expression correlating with resistance to Marek's disease[37,38]. However, structural analyses of high- and low-expressing chicken MHC class I molecules importantly reveal that the width of the peptide-binding groove is large in low-expressing molecules, and narrow in high-expressing MHC class I molecules[37-39]. Similarly, a difference in thermal stability is correlated to surface expression levels[40]. The presentation of peptides on the cell surface of chicken MHC is reliant on the peptide-translocation specificity of TAP, which is known to vary between chicken haplotypes and by TAP polymorphism[39,40]; such peptide-translocation specificity of TAP is not found in humans[41].

Our results, combined with previous work, show that HLA-C expression is modulated by multiple factors acting at several levels, from transcription to miRNA binding and peptide selectivity mediated by the antigen-binding cleft – consequently leading to a net effect that determines abundance at the cell surface (Fig. 10). Such diversity points to a complex evolutionary history. Here, we show that the antigen-binding cleft-encoding sequence of exons 2 and 3 of *C*07*-like alleles has been maintained in primates for millions of years and can be found in modern populations of chimpanzees and other species, while no *C*05*-like alleles were found in the chimpanzee sequences available. By contrast, the 3' miRNA binding site polymorphism seems to have arisen since the split of the human and chimpanzee ancestors, through a gene conversion event from an *HLA-B* sequence[16]. Similarly, there seems to be no evidence for shared polymorphism in the promoter region, likewise indicating that these variants have also arisen since the species diverged[42]. This complex evolutionary and regulatory landscape is suggestive of an ever-changing selective regime, perhaps resulting from transient selection for up- or down-regulation of specific groups of alleles with particular binding specificities, in response to particular pathogens and endogenous factors such as autoimmunity and pregnancy.

METHODS

Transient transfection assays and constructs

The *C*05* and *C*07* hybrid constructs were made by amplifying ~ 2.04 kb and 2.06 kb genomic fragments of *HLA-C*05:01:01:01* and *HLA-C*07:02:01:03* respectively,

which contained 776 bp or 766 bp of the respective *HLA* 5'UTR and exons 1-3 up to a midpoint in intron 3, which was fused to a ~ 3.58 kb fragment of the genomic *H-2K*^{b} gene, beginning at a midpoint in intron 3 and containing exons 4-8 and the *H-2K*^{b} 3'UTR. For experiments with swapped promoters/5'UTR, additional hybrid constructs were made where the 5' flanking region of the HLA genes was interchanged, such that the *HLA-C*05:01:01:01* promoter/5'UTR was fused to the exon 1-3 sequence of *HLA-C*07:02:01:03*, and vice versa. The region from the genomic *H-2K*^{b} gene was the same as described above. These hybrid constructs were transfected into 721.221 cells using optimised electroporation conditions (260V, 1070µF, ∞ resistance) using a Genepulser II (Bio-Rad). A limiting concentration of the pmax-GFP plasmid (Lonza) was co-transfected as a transfection control. The cells were harvested 48 hours post-transfection, and used for flow cytometry or RNA isolation/QPCR experiments. See supplementary information for details.

Luciferase assays

The promoters/5'UTR of *HLA-C*05:01:01:01* (776 bp upstream of the start codon) or *HLA-C*07:02:01:03* (766 bp upstream of the start codon) genes were cloned into a luciferase containing pGL4.14 (Promega) basic promoter-less vector. HEK 293T or 721.221 cells were transfected with the luciferase constructs containing the 5'UTR/promoter from either *C*05*, *C*07* or no promoter, along with the co-transfection of the Renilla luciferase vector, pGL4.74 (Promega), using TransIT 2020 transfection reagent (for HEK 293T cells) or optimised electroporation conditions (for 721.221 cells). Cells were lysed after 24 hours (HEK 293T) or 5 hours (721.221) post-transfection, and firefly and renilla luciferase activities were measured using

dual luciferase reporter assay system (Promega) and the Glomax multi detection system (Promega). The firefly luciferase activity was normalised relative to Renilla luciferase for each transfection, and the luciferase activity of each reporter construct was calculated as a fold change relative to the activity of pGL4.14-basic vector lacking a promoter.

Lentiviral expression assays

The *C*05* and *C*07* lentiviral expression constructs were made by amplifying the cDNA of *HLA-C*05:01:01:01* and *HLA-C*07:02:01:03* genes from exons 1-8, and cloning it into the pHRsinUbEm expression plasmid (a gift from J.M. Boname/ P.J. Lehner, University of Cambridge), with the inclusion of the HA tag at the N-terminus of C*05 and C*07, just after the signal peptide sequence. For the modified *C*05* and *C*07* lentiviral expression constructs, the cDNA of exons 1-3 from the respective *HLA* genes was fused to the cDNA of exons 4-8 of the murine *H-2K*^{b} gene, and cloned into the pHRsinUbEm expression plasmid, with inclusion of the N-terminal HA tag. See supplementary information for details of viral packaging and transduction. Cells were harvested 72 hours post transduction and flow cytometry, RNA isolation/QPCR or immunoblotting experiments were performed.

Statistical analysis

Statistical tests were performed using GraphPad Prism and non-parametric Mann-Whitney U-tests were used for comparing two experimental groups, with a 5% significance level. For swapped promoter analyses, a Bonferroni correction for multiple testing was used; considering P=0.05 for four independent hypotheses, the

significance threshold used for this analyses was *P*=0.0125.

Protein expression, purification and crystallisation

Soluble class I heterodimers of HLA-C*05 and HLA-C*07 heavy chain and full-length β2-microglobulin (β2m) were expressed in *Escherichia coli* as inclusion bodies as previously described[43]. Both HLA molecules were refolded with 4 peptides ITASRFKEL, SAEPVPLQL, RYRPGTVAL and KYFDEHYEY and thermal stability assay was performed as described in the supplementary information.

Crystallisation, data collection and structure determination

Crystals of the HLA-C*05-SAE were grown by the hanging-drop, vapour-diffusion method at 20°C with a protein/reservoir drop ratio of 1:1, at a concentration of 3 mg/mL in 10 mM Tris-HCl pH 8, 150 mM NaCl using 1.8 M Na malonate pH 7. The HLA-C*05:01-SAE crystals were flash frozen in liquid nitrogen. Crystals of HLA-C*0702-RYR were grown in 0.1 M HEPES pH 8.5, 2 mM $ZnSO_4$ and 28 % jeffamine ED-2001 (Hampton), using the same technique as for the HLA-C*05-SAE crystals. The HLA-C*07-RYR crystals were soaked in a mother liquid solution with the addition of 25 % ethylene glycol prior to be flash frozen in liquid nitrogen. The data were collected on the MX1 beamline at the Australian Synchrotron[44], using the ADSC-Quantum 210 CCD detector (at 100K). Data were processed using the XDS[45] and scaled using SCALA software[46] from the CCP4 suite[47]. Details of structures determination and refinement statistics are provided in the supplementary information.

Peptide elution

The HLA class-I negative 721.221 cells stably transfected with HLA-C*05:01 or HLA-C*07:02 were utilised to obtain the peptide repertoires in a previously described manner[48,49]. In short, HLA class I were purified from a total 4 x 10^9 721.221 cells for each HLA-C using the pan class I antibody W6/32 immobilised and cross-linked to protein A resin. Captured HLA-peptide complexes were eluted with 10 % acetic acid. The dissociated complexes were further separated by Reversed-phase HPLC to isolate and fractionate the bound peptides before analysis with a Q Exactive Hybrid Quadrupole-Orbitrap Mass Spectrometer (Thermo Scientific)[49]. Peptides were identified by database search using the human UniProtKB/SwissProt database (Feb 2016) with ProteinPilot V5.0 (SCIEX). A false discovery rate of 5% was applied and known contaminant peptides removed from the final list of peptide ligands. Peptides of 8 – 14 amino acids in length were then used for analysis.

Phylogenetic analysis of human and chimpanzee *HLA-C* alleles

Nucleotide sequences for human and chimpanzee *HLA-C* alleles were obtained from the IMGT database[50]. All chimpanzee sequences in the database were considered and a subset of human sequences was selected in each allele subclass. The region of the sequences aligned included exon 2 and 3 region (without the intron) and spanned 546 bp for the *C*05* and *C*07* sequences. Sequences were aligned with MUSCLE (v3.8.31)[51] and the exon 2 and 3 sequences were extracted from the alignment. MrBayes (v3.2.5)[52] was used to infer the phylogenetic relationship between sequences using the GTR model of nucleotide evolution with rate gamma

distributed, running parameters used were nruns=3, nchains=4, ngen=2000000 and samplefreq=1000.

Generation of heat-map for comparison of regulatory elements in human *HLA-C* alleles

For extended description see supplementary information. In brief, sequences homologous to *HLA-C*05:01:01:01* and *HLA-C*07:02:01:03* were identified in the NCBI nucleotide database using BLAST+ (v. 2.3.0)[53]. Sequences containing the promoter and 5'UTR, exons 2 to 3, and 3'UTR regions were considered for the analysis (details in supplementary information). For display on the heat map, one representative sequence of each allele type was chosen. To quantify the relative similarity between a HLA-C allele and HLA-C*05 and HLA-C*07 in a phylogenetic tree, we calculated a metric quantifying the phylogenetic distance between the query HLA allele and its relative distance to *HLA-C*05* and *HLA-C*07* in the specific tree. Further details of alignments and generation of phylogenetic trees can be found in the supplementary information.

REFERENCES

1 Welter, D. *et al.* The NHGRI GWAS Catalog, a curated resource of SNP-trait associations. *Nucleic Acids Res* **42**, D1001-1006, doi:10.1093/nar/gkt1229 (2014).

2 Parham, P. MHC class I molecules and KIRs in human history, health and survival. *Nat Rev Immunol* **5**, 201-214, doi:10.1038/nri1570 (2005).

3 Shiina, T., Hosomichi, K., Inoko, H. & Kulski, J. K. The HLA genomic loci map: expression, interaction, diversity and disease. *J Hum Genet* **54**, 15-39, doi:10.1038/jhg.2008.5 (2009).

4 Apps, R. *et al.* Influence of HLA-C expression level on HIV control. *Science* **340**, 87-91, doi:10.1126/science.1232685 (2013).

5 Petersdorf, E. W. *et al.* HLA-C expression levels define permissible mismatches in hematopoietic cell transplantation. *Blood* **124**, 3996-4003, doi:10.1182/blood-2014-09-599969 (2014).

6 Koeffler, H. P., Ranyard, J., Yelton, L., Billing, R. & Bohman, R. Gamma-interferon induces expression of the HLA-D antigens on normal and leukemic human myeloid cells. *Proc Natl Acad Sci U S A* **81**, 4080-4084 (1984).

7 Bashirova, A. A., Martin, M. P., McVicar, D. W. & Carrington, M. The killer immunoglobulin-like receptor gene cluster: tuning the genome for defense. *Annu Rev Genomics Hum Genet* **7**, 277-300, doi:10.1146/annurev.genom.7.080505.115726 (2006).

8 Snary, D., Barnstable, C. J., Bodmer, W. F. & Crumpton, M. J. Molecular structure of human histocompatibility antigens: the HLA-C series. *Eur J Immunol* **7**, 580-585, doi:10.1002/eji.1830070816 (1977).

9 Zemmour, J. & Parham, P. Distinctive polymorphism at the HLA-C locus: implications for the expression of HLA-C. *J Exp Med* **176**, 937-950 (1992).

10 Apps, R. *et al.* Relative expression levels of the HLA class-I proteins in normal and HIV-infected cells. *J Immunol* **194**, 3594-3600, doi:10.4049/jimmunol.1403234 (2015).

11 Kulkarni, S. *et al.* Genetic interplay between HLA-C and MIR148A in HIV control and Crohn disease. *Proc Natl Acad Sci U S A* **110**, 20705-20710, doi:10.1073/pnas.1312237110 (2013).

12 Fellay, J. *et al.* A whole-genome association study of major determinants for host control of HIV-1. *Science* **317**, 944-947, doi:10.1126/science.1143767 (2007).

13 Kulkarni, S. *et al.* Differential microRNA regulation of HLA-C expression and its association with HIV control. *Nature* **472**, 495-498, doi:10.1038/nature09914 (2011).

14 Thomas, R. *et al.* HLA-C cell surface expression and control of HIV/AIDS correlate with a variant upstream of HLA-C. *Nat Genet* **41**, 1290-1294, doi:10.1038/ng.486 (2009).

15 Apps, R. *et al.* HIV-1 Vpu Mediates HLA-C Downregulation. *Cell Host Microbe* **19**, 686-695, doi:10.1016/j.chom.2016.04.005 (2016).

16 O'Huigin, C. *et al.* The molecular origin and consequences of escape from miRNA regulation by HLA-C alleles. *Am J Hum Genet* **89**, 424-431, doi:10.1016/j.ajhg.2011.07.024 (2011).

17 Pereyra, F. *et al.* The major genetic determinants of HIV-1 control affect HLA class I peptide presentation. *Science* **330**, 1551-1557, doi:10.1126/science.1195271 (2010).

18 Gonzalez-Galarza, F. F. *et al.* Allele frequency net 2015 update: new features for HLA epitopes, KIR and disease and HLA adverse drug reaction associations. *Nucleic Acids Res* **43**, D784-788, doi:10.1093/nar/gku1166 (2015).

19 Borenstein, S. H., Graham, J., Zhang, X. L. & Chamberlain, J. W. CD8+ T cells are necessary for recognition of allelic, but not locus-mismatched or xeno-, HLA class I transplantation antigens. *J Immunol* **165**, 2341-2353 (2000).

20 Hundhausen, C. *et al.* Allele-specific cytokine responses at the HLA-C locus: implications for psoriasis. *J Invest Dermatol* **132**, 635-641, doi:10.1038/jid.2011.378 (2012).

21 Apps, R. *et al.* Human leucocyte antigen (HLA) expression of primary trophoblast cells and placental cell lines, determined using single antigen beads to characterize allotype specificities of anti-HLA antibodies. *Immunology* **127**, 26-39, doi:10.1111/j.1365-2567.2008.03019.x (2009).

22 Hilton, H. G. & Parham, P. Direct binding to antigen-coated beads refines the specificity and cross-reactivity of four monoclonal antibodies that recognize polymorphic epitopes of HLA class I molecules. *Tissue Antigens* **81**, 212-220, doi:10.1111/tan.12095 (2013).

23 Kim, E., Kwak, H. & Ahn, K. Cytosolic aminopeptidases influence MHC class I-mediated antigen presentation in an allele-dependent manner. *J Immunol* **183**, 7379-7387, doi:10.4049/jimmunol.0901489 (2009).

24 Neisig, A., Melief, C. J. & Neefjes, J. Reduced cell surface expression of HLA-C molecules correlates with restricted peptide binding and stable TAP interaction. *J Immunol* **160**, 171-179 (1998).

25 Sibilio, L. *et al.* A single bottleneck in HLA-C assembly. *J Biol Chem* **283**, 1267-1274, doi:10.1074/jbc.M708068200 (2008).

26 Addo, M. M. *et al.* The HIV-1 regulatory proteins Tat and Rev are frequently targeted by cytotoxic T lymphocytes derived from HIV-1-infected individuals. *Proc Natl Acad Sci U S A* **98**, 1781-1786, doi:10.1073/pnas.98.4.1781 (2001).

27 Vales-Gomez, M., Reyburn, H. T., Mandelboim, M. & Strominger, J. L. Kinetics of interaction of HLA-C ligands with natural killer cell inhibitory receptors. *Immunity* **9**, 337-344 (1998).

28 Rasmussen, M. *et al.* Uncovering the peptide-binding specificities of HLA-C: a general strategy to determine the specificity of any MHC class I molecule. *J Immunol* **193**, 4790-4802, doi:10.4049/jimmunol.1401689 (2014).

29 Hofmann, S. *et al.* Rapid and sensitive identification of major histocompatibility complex class I-associated tumor peptides by Nano-LC MALDI MS/MS. *Mol Cell Proteomics* **4**, 1888-1897, doi:10.1074/mcp.M500076-MCP200 (2005).

30 Falk, K. *et al.* Allele-specific peptide ligand motifs of HLA-C molecules. *Proc Natl Acad Sci U S A* **90**, 12005-12009 (1993).

31 Miyadera, H., Ohashi, J., Lernmark, A., Kitamura, T. & Tokunaga, K. Cell-surface MHC density profiling reveals instability of autoimmunity-associated HLA. *J Clin Invest* **125**, 275-291, doi:10.1172/JCI74961 (2015).

32 Reits, E. A. *et al.* Radiation modulates the peptide repertoire, enhances MHC class I expression, and induces successful antitumor immunotherapy. *J Exp Med* **203**, 1259-1271, doi:10.1084/jem.20052494 (2006).

33 Faroudi, M. *et al.* Lytic versus stimulatory synapse in cytotoxic T lymphocyte/target cell interaction: manifestation of a dual activation threshold. *Proc Natl Acad Sci U S A* **100**, 14145-14150, doi:10.1073/pnas.2334336100 (2003).

34 Thomas, R. *et al.* A novel variant marking HLA-DP expression levels predicts recovery from hepatitis B virus infection. *J Virol* **86**, 6979-6985, doi:10.1128/JVI.00406-12 (2012).

35 Cassidy, S. A., Cheent, K. S. & Khakoo, S. I. Effects of Peptide on NK cell-mediated MHC I recognition. *Front Immunol* **5**, 133, doi:10.3389/fimmu.2014.00133 (2014).

36 Blais, M. E., Dong, T. & Rowland-Jones, S. HLA-C as a mediator of natural killer and T-cell activation: spectator or key player? *Immunology* **133**, 1-7, doi:10.1111/j.1365-2567.2011.03422.x (2011).

37 Chappell, P. *et al.* Expression levels of MHC class I molecules are inversely correlated with promiscuity of peptide binding. *Elife* **4**, e05345, doi:10.7554/eLife.05345 (2015).

38 Koch, M. *et al.* Structures of an MHC class I molecule from B21 chickens illustrate promiscuous peptide binding. *Immunity* **27**, 885-899, doi:10.1016/j.immuni.2007.11.007 (2007).

39 Zhang, J. *et al.* Narrow groove and restricted anchors of MHC class I molecule BF2*0401 plus peptide transporter restriction can explain disease susceptibility of B4 chickens. *J Immunol* **189**, 4478-4487, doi:10.4049/jimmunol.1200885 (2012).

40 Tregaskes, C. A. *et al.* Surface expression, peptide repertoire, and thermostability of chicken class I molecules correlate with peptide transporter specificity. *Proc Natl Acad Sci U S A* **113**, 692-697, doi:10.1073/pnas.1511859113 (2016).

41 Obst, R., Armandola, E. A., Nijenhuis, M., Momburg, F. & Hammerling, G. J. TAP polymorphism does not influence transport of peptide variants in mice and humans. *Eur J Immunol* **25**, 2170-2176, doi:10.1002/eji.1830250808 (1995).

42 Auton, A. *et al.* A fine-scale chimpanzee genetic map from population sequencing. *Science* **336**, 193-198, doi:10.1126/science.1216872 (2012).

43 Gras, S. *et al.* The shaping of T cell receptor recognition by self-tolerance. *Immunity* **30**, 193-203, doi:10.1016/j.immuni.2008.11.011 (2009).

44 Cowieson, N. P. *et al.* MX1: a bending-magnet crystallography beamline serving both chemical and macromolecular crystallography communities at the Australian Synchrotron. *J Synchrotron Radiat* **22**, 187-190, doi:10.1107/S1600577514021717 (2015).

45 Kabsch, W. Xds. *Acta Crystallogr D Biol Crystallogr* **66**, 125-132, doi:10.1107/S0907444909047337 (2010).

46 Evans, P. Scaling and assessment of data quality. *Acta Crystallogr D Biol Crystallogr* **62**, 72-82, doi:10.1107/S0907444905036693 (2006).

47 Collaborative Computational Project, N. The CCP4 suite: programs for protein crystallography. *Acta Crystallogr D Biol Crystallogr* **50**, 760-763, doi:10.1107/S0907444994003112 (1994).

48 Schittenhelm, R. B., Dudek, N. L., Croft, N. P., Ramarathinam, S. H. & Purcell, A. W. A comprehensive analysis of constitutive naturally processed and presented HLA-C*04:01 (Cw4)-specific peptides. *Tissue Antigens* **83**, 174-179, doi:10.1111/tan.12282 (2014).

49 Dudek, N. L., Croft, N. P., Schittenhelm, R. B., Ramarathinam, S. H. & Purcell, A. W. A Systems Approach to Understand Antigen Presentation and the Immune Response. *Methods Mol Biol* **1394**, 189-209, doi:10.1007/978-1-4939-3341-9_14 (2016).

50 Robinson, J. *et al.* The IPD and IMGT/HLA database: allele variant databases. *Nucleic Acids Res* **43**, D423-431, doi:10.1093/nar/gku1161 (2015).

51 Edgar, R. C. MUSCLE: multiple sequence alignment with high accuracy and high throughput. *Nucleic Acids Res* **32**, 1792-1797, doi:10.1093/nar/gkh340 (2004).

52 Ronquist, F. *et al.* MrBayes 3.2: efficient Bayesian phylogenetic inference and model choice across a large model space. *Syst Biol* **61**, 539-542, doi:10.1093/sysbio/sys029 (2012).

53 Camacho, C. *et al.* BLAST+: architecture and applications. *BMC Bioinformatics* **10**, 421, doi:10.1186/1471-2105-10-421 (2009).

54 Dundas, J. *et al.* CASTp: computed atlas of surface topography of proteins with structural and topographical mapping of functionally annotated residues. *Nucleic Acids Res* **34**, W116-118, doi:10.1093/nar/gkl282 (2006).

ACKNOWLEDGEMENTS

We would like to acknowledge the flow cytometry facility at the WIMM, which is supported by the MRC HIU; MRC MHU (MC_UU_12009); NIHR Oxford BRC and John Fell Fund (131/030 and 101/517), the EPA fund (CF182 and CF170) and by the WIMM Strategic Alliance awards G0902418 and MC_UU_12025. We would also like to acknowledge use of the facilities and the assistance of Dr. Ralf Schittenhelm at the

Monash Biomedical Proteomics Facility. Work in the authors' laboratories is supported by the UK and Danish Medical Research Councils, The Lundbeck Foundation, The Alan and Babette Sainsbury Charitable Fund, the Naomi Bramson Trust, the Clinical Neuroimmunology Fund, the Oxford Biomedical Research Centre, the Oak Foundation (L.F.), Wellcome Trust (100308/Z/12/Z and 106130/Z/14/Z, L.F.; 100956/Z/13/Z, G.M.), Australian National Health and Medical Research Council (NHMRC), Australian Research Council (ARC) (J.R., A.W.P.), ARC Laureate fellowship (J.R.), NHMRC Senior Research Fellowship (1044215, A.W.P.), ARC Future Fellowship (FT120100416, S.G.). This project has been funded in part with federal funds from the Frederick National Laboratory for Cancer Research, under Contract No. HHSN261200800001E. This Research was supported in part by the Intramural Research Program of the NIH, Frederick National Lab, Center for Cancer Research.

AUTHOR CONTRIBUTIONS

G.K. contributed to conception, coordination and design of the study, all experiments apart from the protein crystallisation and structural work, and to data analyses, drafting and writing of the manuscript. S.G. contributed to all structural experiments including protein purifications, stability assays, crystallisations and structure determination, and to writing of the manuscript. J.I.M. contributed to structural experiments including protein purifications, crystallisations, structure determination, and peptide repertoire analysis, and to writing of the manuscript. J.P.V contributed to structural experiments including protein purifications, crystallisations, structure determination, and peptide repertoire analysis. A.C. performed all phylogenetic

analyses of human and chimpanzee sequences, and contributed to writing of the manuscript. T.B. contributed to cloning of HLA-C constructs, cellular transfection experiments, flow cytometry, QPCR, and data analyses. S.B.K. contributed to optimisation of QPCR experiments. L.T.J. contributed to cloning of HLA-C genomic constructs. K.E.A. contributed to experimental design and manuscript editing. C.D. contributed to experimental design, data and analyses discussions, and to manuscript editing. M.C. provided intellectual input and contributed to manuscript editing. G.M. contributed to the conception and design of phylogenetic analyses and to writing of the manuscript. A.W.P. contributed to conception and design of the peptide repertoire analyses. J.R. contributed to the conception and design of the structural work and to writing of the manuscript. L.F. contributed to conception, coordination and design of the study, and drafting and writing of the manuscript.

COMPETING FINANCIAL INTEREST: The authors declare no competing financial interests

DISCLAIMER: The content of this publication does not necessarily reflect the views or policies of the Department of Health and Human Services, nor does mention of trade names, commercial products, or organizations imply endorsement by the U.S. Government.

FIGURE LEGENDS

Fig. 1 - Differential expression of HLA-C*05 and HLA-C*07

(**a**) Schematic representation of *C*05* (red) and *C*07* (blue) genomic constructs; construct design is detailed in the methods, murine *H-2K*^{b} gene is shown in grey. (**b**) Representative cell surface expression of HLA-C on 721.221 cells transfected with the *C*05* and *C*07* genomic constructs. HLA-C (W6/32) staining is shown on GFP+ cells. C*05 (red), C*07 (blue) and vector transfected cells (black) are shown. Numbers denote mean fluorescence intensity (MFI) of HLA-C+GFP+ cells. (**c**) Normalised HLA-C (W6/32) expression on GFP+ C*05 and C*07 transfected 721.221 cells. MFI of W6/32 on the gated HLA-C+GFP+ population/MFI of GFP on GFP+ cells is plotted, and shown relative to C*07 transfected cells. Mean ± S.E.M is depicted, n=9.

Fig. 2 – The promoter/5'UTR of *HLA-C*05* and *HLA-C*07* differentially affects expression of the luciferase reporter gene, but does not directly impact differential cell surface expression of HLA-C

(**a**) Schematic representation of the luciferase reporter constructs; construct design is detailed in the methods. Luciferase reporter constructs were transfected into (**b**) HEK 293T cells, and (**c**) 721.221 cells, and dual luciferase reporter assays performed on cell lysates. Relative light units (RLU) plotted as fold change in luciferase activity of the promoter/5'UTR of the *HLA-C* alleles compared to empty-vector is shown. (**d**) Schematic representation of the *C*05* and *C*07* genomic constructs with or without the swapped promoter/5'UTR. (**e**) Representative cell surface expression of HLA-C on 721.221 cells transfected with the *C*05* and *C*07* genomic constructs. HLA-C (W6/32) staining is shown on GFP+ cells. Histogram colour coding is indicated in the panel **d**, black line represents vector-transfected cells, numbers denote MFI. (**f**)

Normalised HLA-C (W6/32) expression on GFP+ *C*05* and *C*07* transfected 721.221 cells. MFI of W6/32 on the gated HLA-C+ GFP+ population/MFI of GFP on GFP+ cells is plotted, and shown relative to *C*07* transfected cells. Mean ± S.E.M is depicted, (**b**) n=12, (**c**) n=9, (**e, f**) n=6-9.

Fig. 3 – Lentiviral expression of HLA-C*05 and HLA-C*07 using exonic constructs preserves the expression pattern of HLA-C molecules

(**a**) Schematic representation of the HA-tagged *C*05* and *C*07* lentiviral constructs which include the sequence of exon 1-8 from the respective *HLA-C* alleles; HLA-C expression is driven by a common SFFV lentiviral promoter. Representative cell surface expression of HLA-C on 721.221 cells transduced with the lentiviral *C*05* and *C*07* constructs. (**b**) HLA-C (W6/32) staining and (**c**) HLA-C (HA) staining is shown on GFP+ cells. *C*05* (red), *C*07* (blue) and vector transduced cells (black) are shown, numbers denote MFI (**d**) Normalised HLA-C (W6/32) expression and (**e**) HLA-C (HA) expression on GFP+ *C*05* and *C*07* transduced 721.221 cells. MFI of W6/32 or HA/MFI of GFP, on the GFP+ population is plotted, and shown relative to *C*07* transduced cells. Mean ± S.E.M is depicted, n=6.

Fig. 4 – Variation in exons 2-3 (α1/α2 domains) of *HLA-C* is responsible for differential expression of C*05 and C*07

(**a**) Schematic representation of the modified HA-tagged *C*05* and *C*07* lentiviral constructs which include the sequence of exons 1-3 from the respective *HLA-C* alleles, and sequence of exon 4 – exon 8 of the murine *H-2K^b* gene; HLA-C expression is driven by a common SFFV lentiviral promoter. Representative cell

surface expression of HLA-C on 721.221 cells transduced with the modified lentiviral C*05 and C*07 constructs. (**b**) HLA-C (W6/32) staining and (**c**) HLA-C (HA) staining is shown on GFP+ cells. *C*05* (red), *C*07* (blue) and vector transduced cells (black) are shown, numbers denote MFI. (**d**) Normalised HLA-C (W6/32) expression and (**e**) HLA-C (HA) expression on GFP+ *C*05* and *C*07* transduced 721.221 cells. MFI of W6/32 or HA/MFI of GFP, on the GFP+ population is plotted, and shown relative to *C*07* transduced cells. Mean ± S.E.M is depicted, n=9-11.

Fig. 5 – Peptide-HLA-C interactions

The panels (**a**-**d**) represent the interaction of the HLA-C*05 molecule (red) with the SAE peptide (gray sticks), with the residues involved in the interaction represented as stick. The panels (**e**, **f**) represent the interaction of the HLA-C*07 molecule (blue) with the RYR peptide (orange). The black dashed lines represent the interaction between the peptide and HLA molecule. (**g**) HLA-C*05 α1/α2 domains structure represented in cartoon (red) with the polymorphic residues that differ with HLA-C*07 coloured in green.

Fig. 6 – Structural comparison of HLA-C*05 and HLA-C*07

Panels (**a**, **b**) represent the HLA-C*05 structure (red) or the HLA-C*07 (blue) based on the HLA-C*05 structure in the same orientation. Panel (**c**) shows the superposition of the HLA-C*05 and HLA-C*07 structures, coloured as red and blue, respectively. (**d, e**) Panels show a surface representation of the antigen-binding cleft of HLA-C*05 (red) and of the HLA-C*07 (blue), calculated using CASTp web server[54].

Fig. 7 – Comparison of peptide repertoire of HLA-C*05 and HLA-C*07

Peptide length analysis of (a) HLA-C*05:01 and (b) HLA-C*07:02 transfected 721.221 cells. Peptide motifs identified for nonamers for (c) HLA-C*05:01 and (d) HLA-C*07:02 are shown. Residues identified as dominant occur at a frequency of > 30 %, strong > 20% and preferred > 10 %.

Fig. 8 - Phylogenetic analysis of human *HLA-C* and chimpanzee *MHC-C* sequences in the exons 2 and 3 region

HLA-C exon 2 and exon 3 sequences were aligned and used to infer phylogenetic relationship. Nodes are labelled with the estimated posterior for each split in the tree. The scale represents expected substitutions per site. *HLA-C*05:01:01:01* (red), *HLA-C*07:02:01:03* (blue), other *HLA-C* alleles (black) and chimpanzee *Patr-C* alleles (black bold) are shown.

Fig. 9 - Patterns of genetic diversity in human *HLA-C* alleles at three regulatory sites

Each grid represents the similarity between a *HLA-C* allele and the *HLA-C*05:01:01:01* and *HLA-C*07:02:01:03* alleles, and it is coloured based on its similarity to *C*05*. Similarity is determined through phylogenetic analysis at the promoter/5'UTR, exon 2-3, and 3'UTR regions. The display of HLA-C subgroup alleles is based on their similarity ranking in the exon 2-3 region. Inferred trees utilised to extract these similarities are presented in Supplementary Fig. 6.

Fig. 10 - The regulatory landscape of HLA-C expression

A combination of variants in the 5'UTR, the antigen-binding cleft, and the 3'UTR, and potentially other yet unidentified factors, drive differential HLA-C expression at the cell-surface.

Figure 1

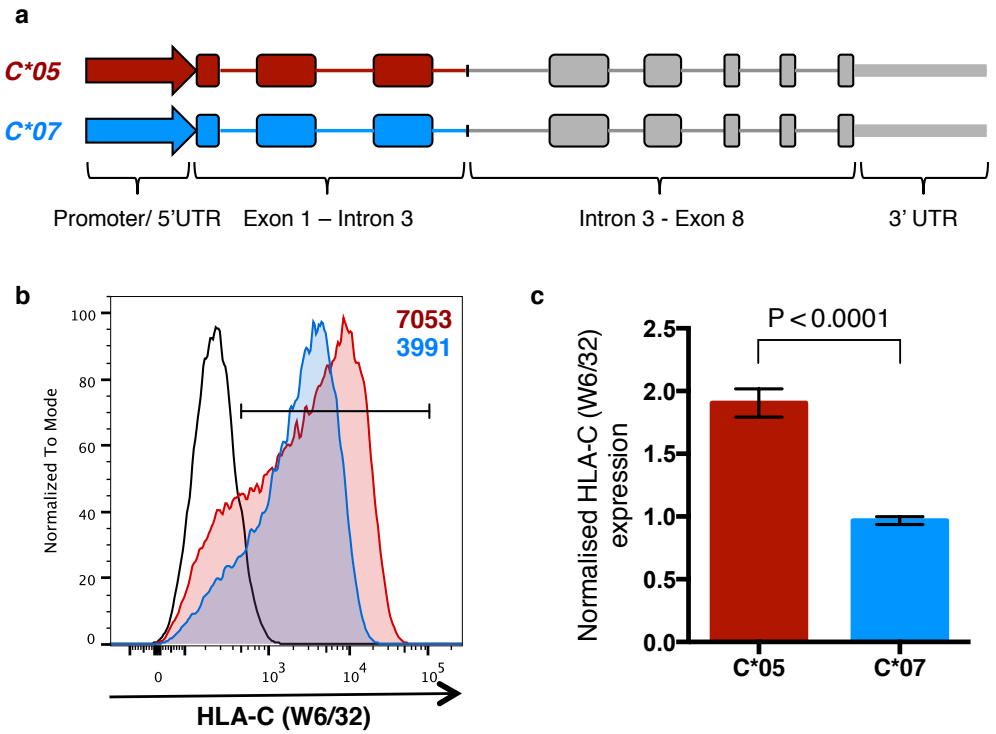

Fig. 1 - Differential expression of HLA-C*05 and HLA-C*07

(**a**) Schematic representation of *C*05* (red) and *C*07* (blue) genomic constructs; construct design is detailed in the methods, murine *H-2K^b* gene is shown in grey. (**b**) Representative cell surface expression of HLA-C on 721.221 cells transfected with the *C*05* and *C*07* genomic constructs. HLA-C (W6/32) staining is shown on GFP+ cells. C*05 (red), C*07 (blue) and vector transfected cells (black) are shown. Numbers denote mean fluorescence intensity (MFI) of HLA-C+GFP+ cells. (**c**) Normalised HLA-C (W6/32) expression on GFP+ C*05 and C*07 transfected 721.221 cells. MFI of W6/32 on the gated HLA-C +GFP+ population/MFI of GFP on GFP+ cells is plotted, and shown relative to C*07 transfected cells. Mean ± S.E.M is depicted, n=9.

Figure 2

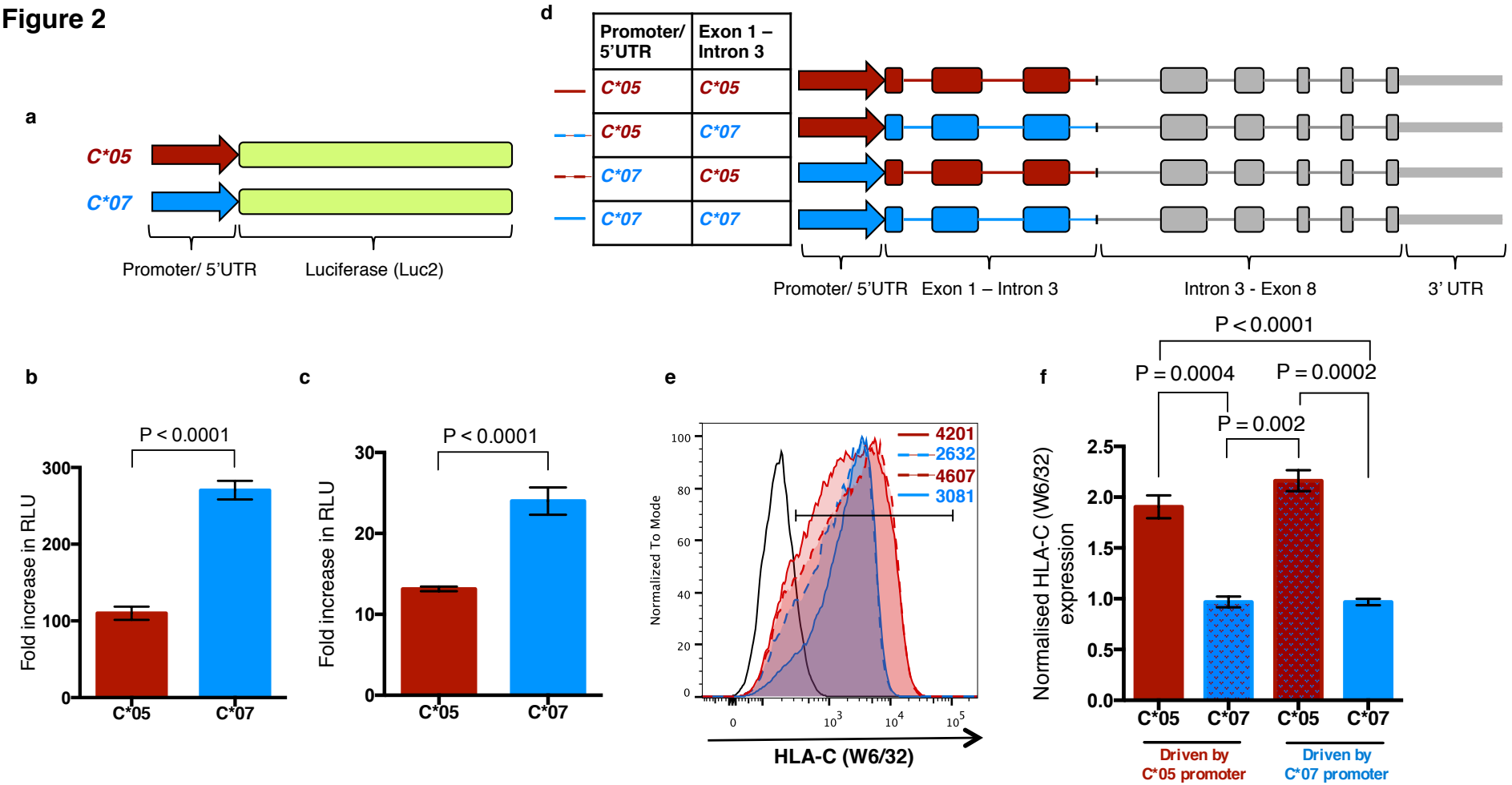

Fig. 2 – The promoter/5'UTR of *HLA-C*05* and *HLA-C*07* differentially affects expression of the luciferase reporter gene, but does not directly impact differential cell surface expression of HLA-C

(**a**) Schematic representation of the luciferase reporter constructs; construct design is detailed in the methods. Luciferase reporter constructs were transfected into (**b**) HEK 293T cells, and (**c**) 721.221 cells, and dual luciferase reporter assays performed on cell lysates. Relative light units (RLU) plotted as fold change in luciferase activity of the promoter/5'UTR of the *HLA-C* alleles compared to empty-vector is shown. (**d**) Schematic representation of the *C*05* and *C*07* genomic constructs with or without the swapped promoter/5'UTR. (**e**) Representative cell surface expression of HLA-C on 721.221 cells transfected with the *C*05* and *C*07* genomic constructs. HLA-C (W6/32) staining is shown on GFP+ cells. Histogram colour coding is indicated in the panel **d**, black line represents vector-transfected cells, numbers denote MFI. (**f**) Normalised HLA-C (W6/32) expression on GFP+ *C*05* and *C*07* transfected 721.221 cells. MFI of W6/32 on the gated HLA-C+ GFP+ population/MFI of GFP on GFP+ cells is plotted, and shown relative to *C*07* transfected cells. Mean ± S.E.M is depicted, (**b**) n=12, (**c**) n=9, (**e, f**) n=6-9.

Figure 3

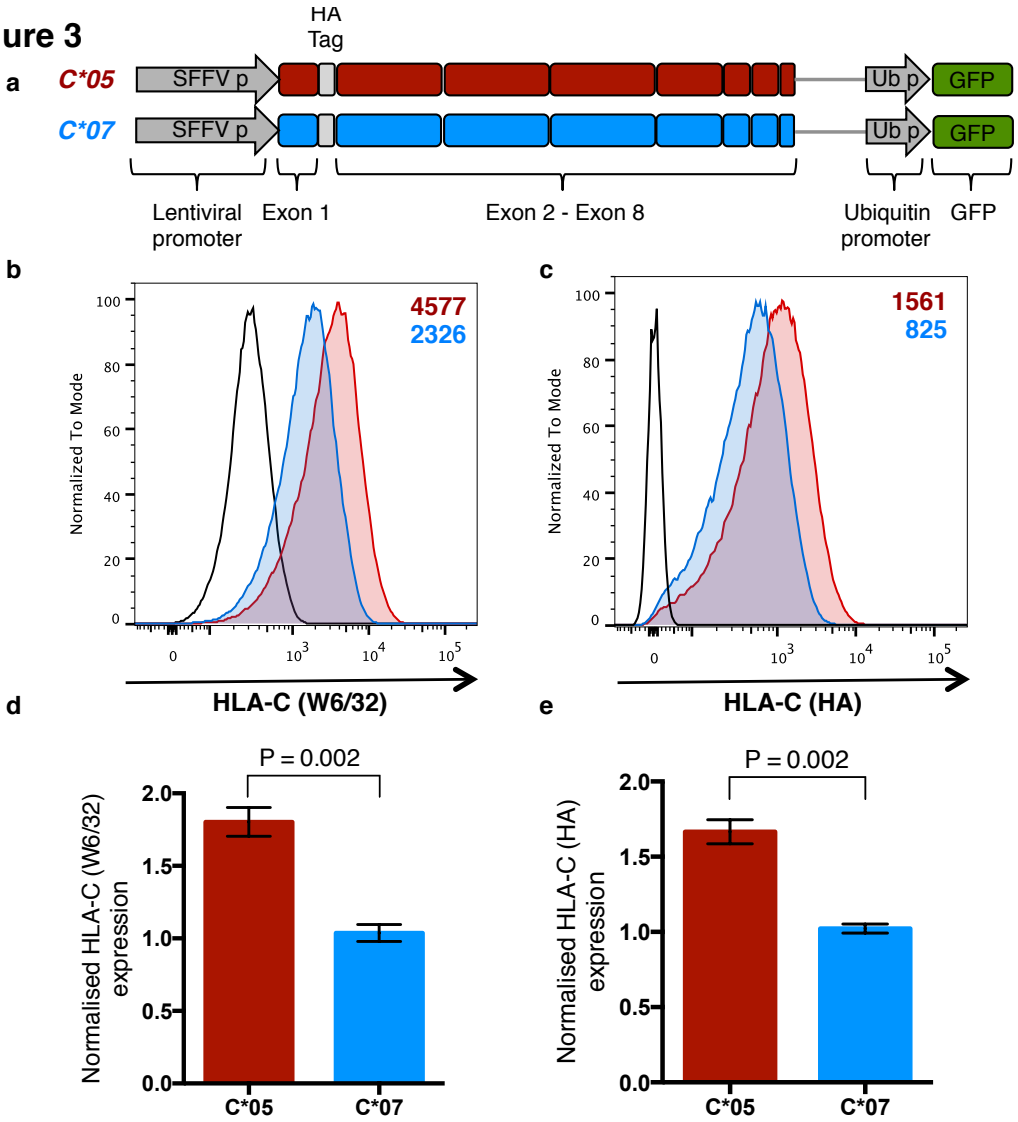

Fig. 3 – Lentiviral expression of HLA-C*05 and HLA-C*07 using exonic constructs preserves the expression pattern of HLA-C molecules

(**a**) Schematic representation of the HA-tagged *C*05* and *C*07* lentiviral constructs which include the sequence of exon 1-8 from the respective *HLA-C* alleles; HLA-C expression is driven by a common SFFV lentiviral promoter. Representative cell surface expression of HLA-C on 721.221 cells transduced with the lentiviral *C*05* and *C*07* constructs. (**b**) HLA-C (W6/32) staining and (**c**) HLA-C (HA) staining is shown on GFP+ cells. *C*05* (red), *C*07* (blue) and vector transduced cells (black) are shown, numbers denote MFI (**d**) Normalised HLA-C (W6/32) expression and (**e**) HLA-C (HA) expression on GFP+ *C*05* and *C*07* transduced 721.221 cells. MFI of W6/32 or HA/MFI of GFP, on the GFP+ population is plotted, and shown relative to *C*07* transduced cells. Mean ± S.E.M is depicted, n=6.

Figure 4

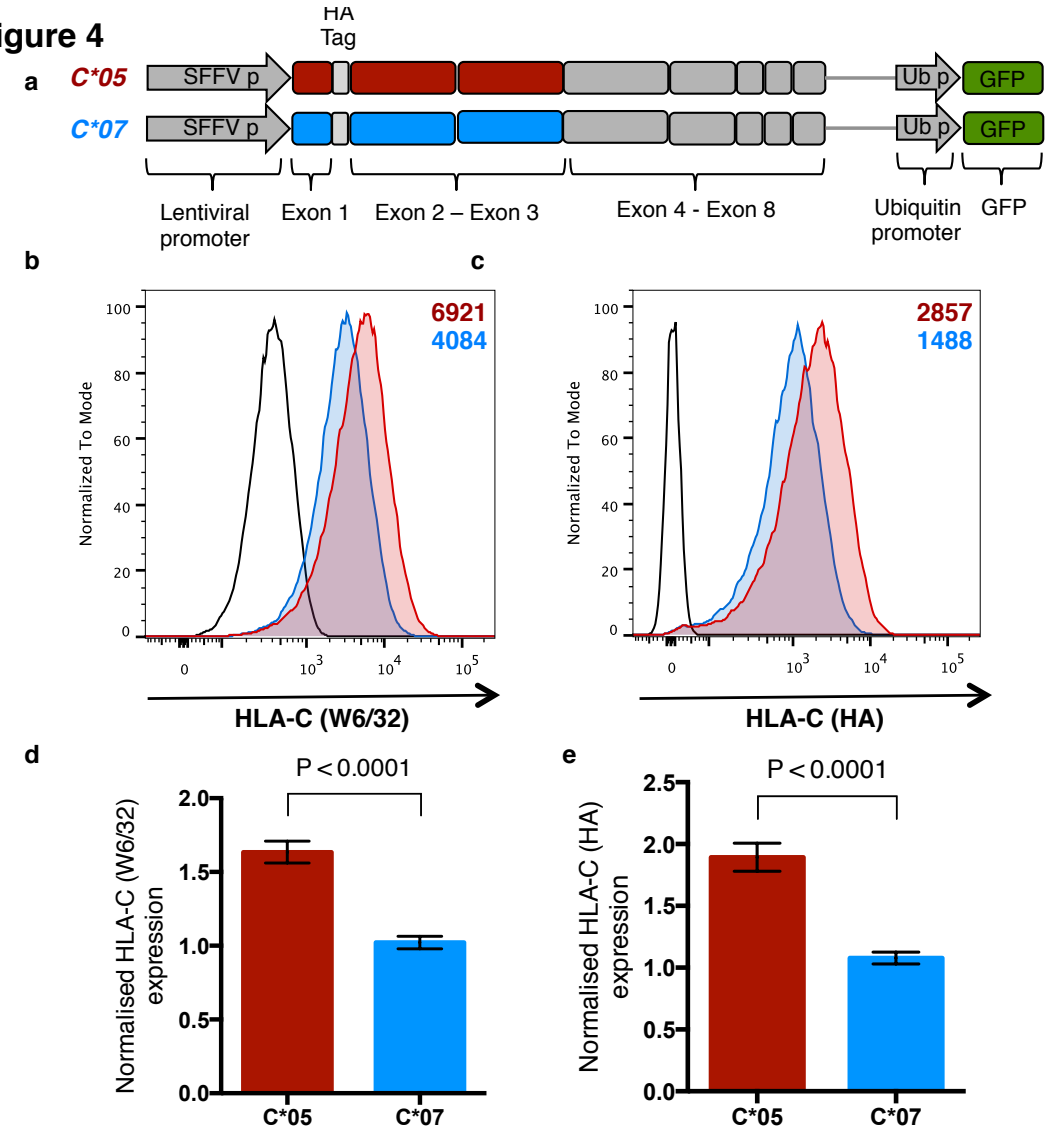

Fig. 4 – Variation in exons 2-3 (α1/α2 domains) of *HLA-C* is responsible for differential expression of C*05 and C*07

(**a**) Schematic representation of the modified HA-tagged *C*05* and *C*07* lentiviral constructs which include the sequence of exons 1-3 from the respective *HLA-C* alleles, and sequence of exon 4 – exon 8 of the murine *H-2K^b* gene; HLA-C expression is driven by a common SFFV lentiviral promoter. Representative cell surface expression of HLA-C on 721.221 cells transduced with the modified lentiviral C*05 and C*07 constructs. (**b**) HLA-C (W6/32) staining and (**c**) HLA-C (HA) staining is shown on GFP+ cells. *C*05* (red), *C*07* (blue) and vector transduced cells (black) are shown, numbers denote MFI. (**d**) Normalised HLA-C (W6/32) expression and (**e**) HLA-C (HA) expression on GFP+ *C*05* and *C*07* transduced 721.221 cells. MFI of W6/32 or HA/MFI of GFP, on the GFP+ population is plotted, and shown relative to *C*07* transduced cells. Mean ± S.E.M is depicted, n=9-11.

Figure 5

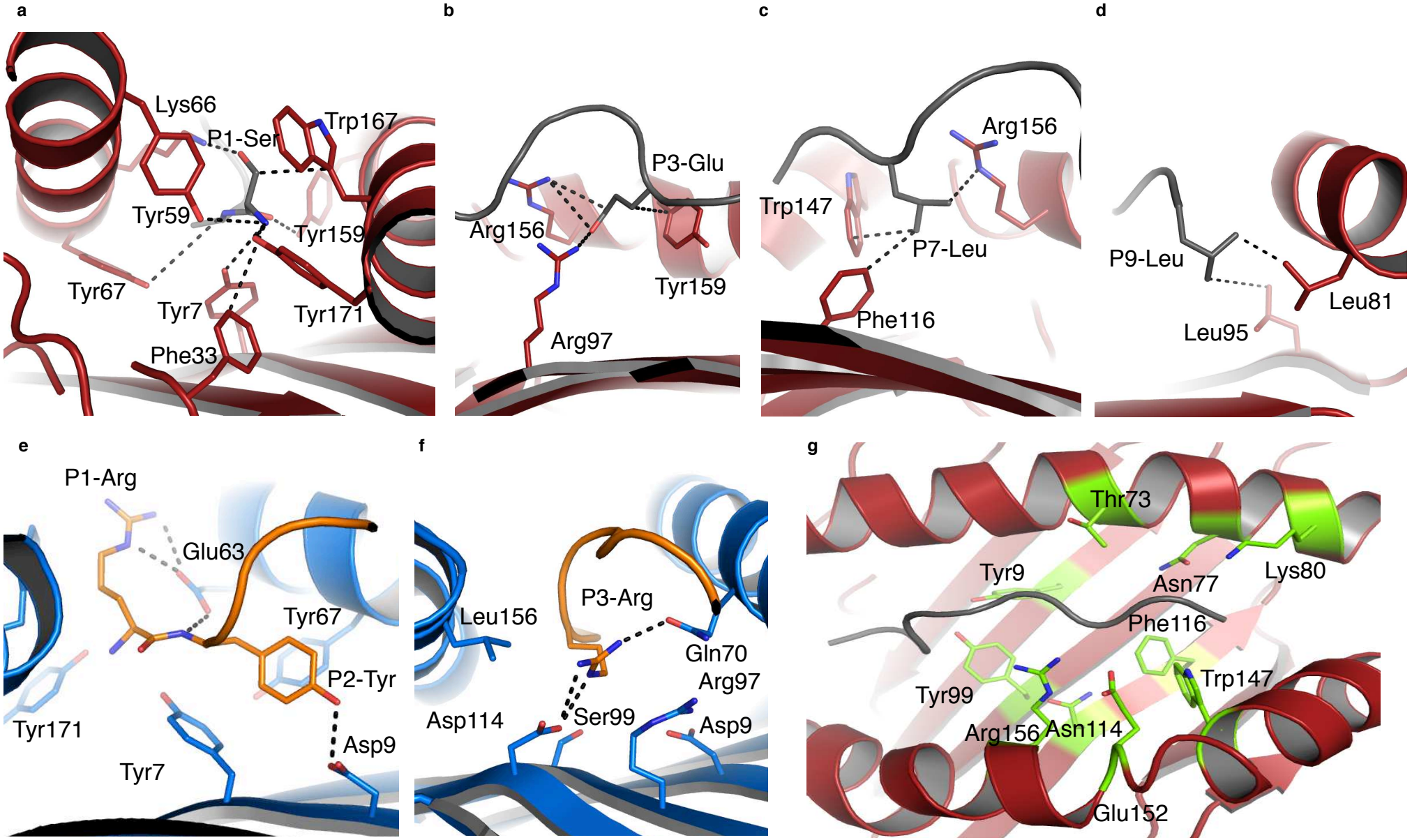

Fig. 5 – Peptide-HLA-C interactions

The panels (**a-d**) represent the interaction of the HLA-C*05 molecule (red) with the SAE peptide (gray sticks), with the residues involved in the interaction represented as stick. The panels (**e, f**) represent the interaction of the HLA-C*07 molecule (blue) with the RYR peptide (orange). The black dashed lines represent the interaction between the peptide and HLA molecule. (**g**) HLA-C*05 α1/α2 domains structure represented in cartoon (red) with the polymorphic residues that differ with HLA-C*07 coloured in green.

Figure 6

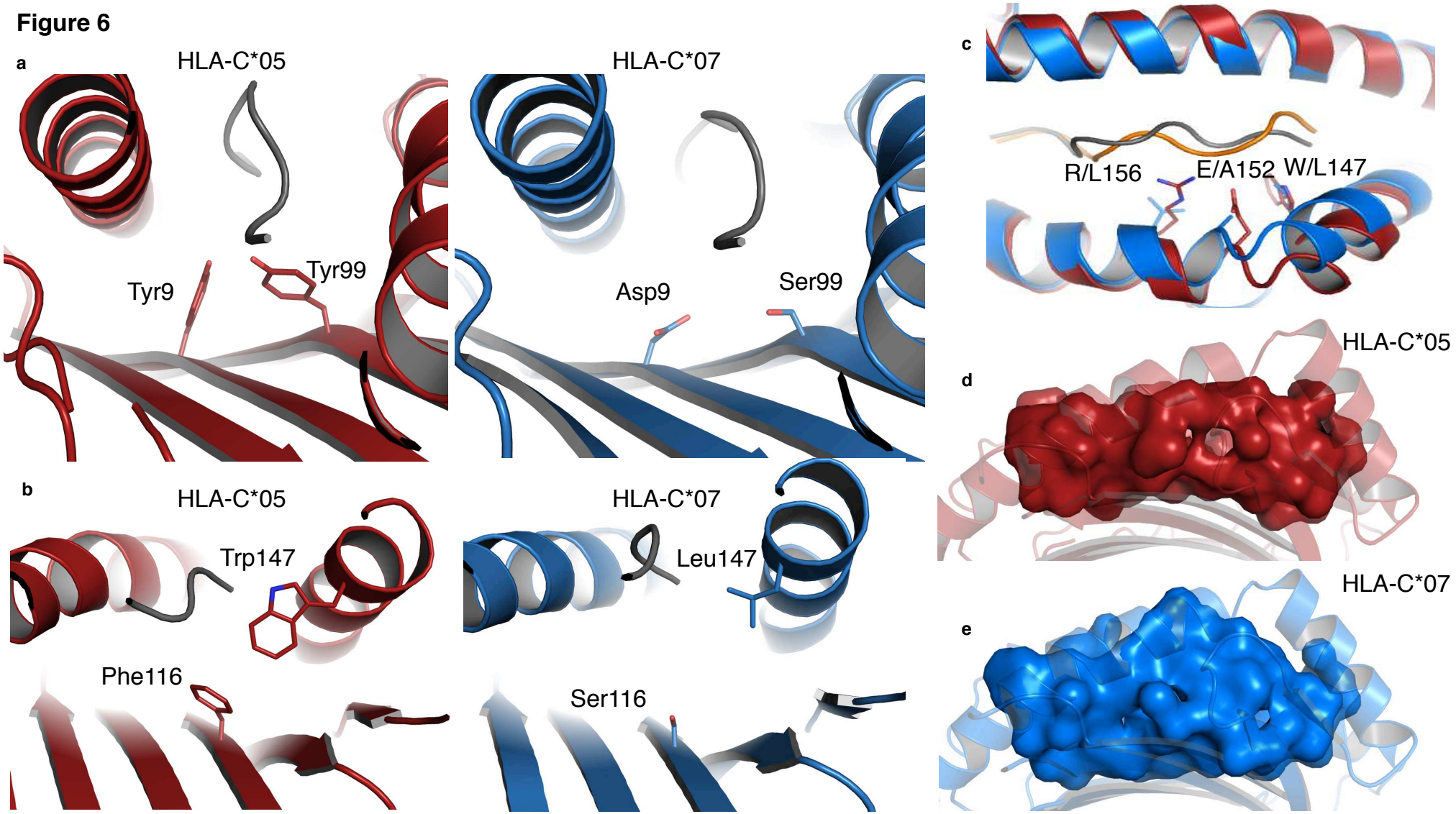

Fig. 6 – Structural comparison of HLA-C*05 and HLA-C*07

Panels (**a**, **b**) represent the HLA-C*05 structure (red) or the HLA-C*07 (blue) based on the HLA-C*05 structure in the same orientation. Panel (**c**) shows the superposition of the HLA-C*05 and HLA-C*07 structures, colour as red and blue, respectively. (**d, e**) Panels show a surface representation of the antigen-binding cleft of HLA-C*05 (red) and of the HLA-C*07 (blue) respectively, calculated using CASTp web server[50].

Figure 7

a

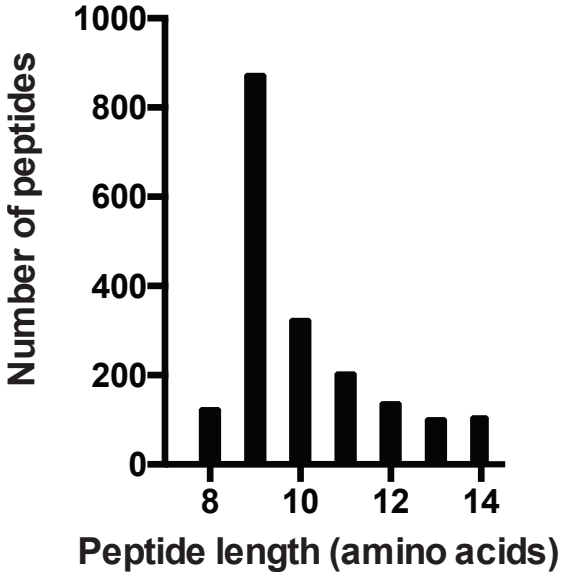

b

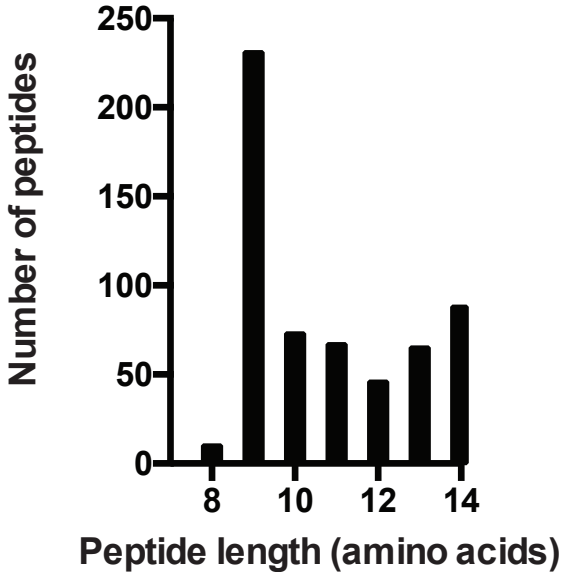

c

HLA-C*05:01 Nonamers

	P1	P2	P3	P4	P5	P6	P7	P8	P9
Dominant		A	D						L
Strong								K	
Preferred	S F A V	S V	E	E D K	K	V	V S		F M V

Total = 873

d

HLA-C*07:02 Nonamers

	P1	P2	P3	P4	P5	P6	P7	P8	P9
Dominant		R Y							L Y
Strong									
Preferred	F Y V	K	P V	P D E	V Y	V P	F L	E S T	F M

Total = 231

Fig. 7 – Comparison of peptide repertoire of HLA-C*05 and HLA-C*07

Peptide length analysis of (a) HLA-C*05:01 and (b) HLA-C*07:02 transfected 721.221 cells. Peptide motifs identified for nonamers for (c) HLA-C*05:01 and (d) HLA-C*07:02 are shown. Residues identified as dominant occur at a frequency of > 30 %, strong > 20% and preferred > 10 %.

Figure 8

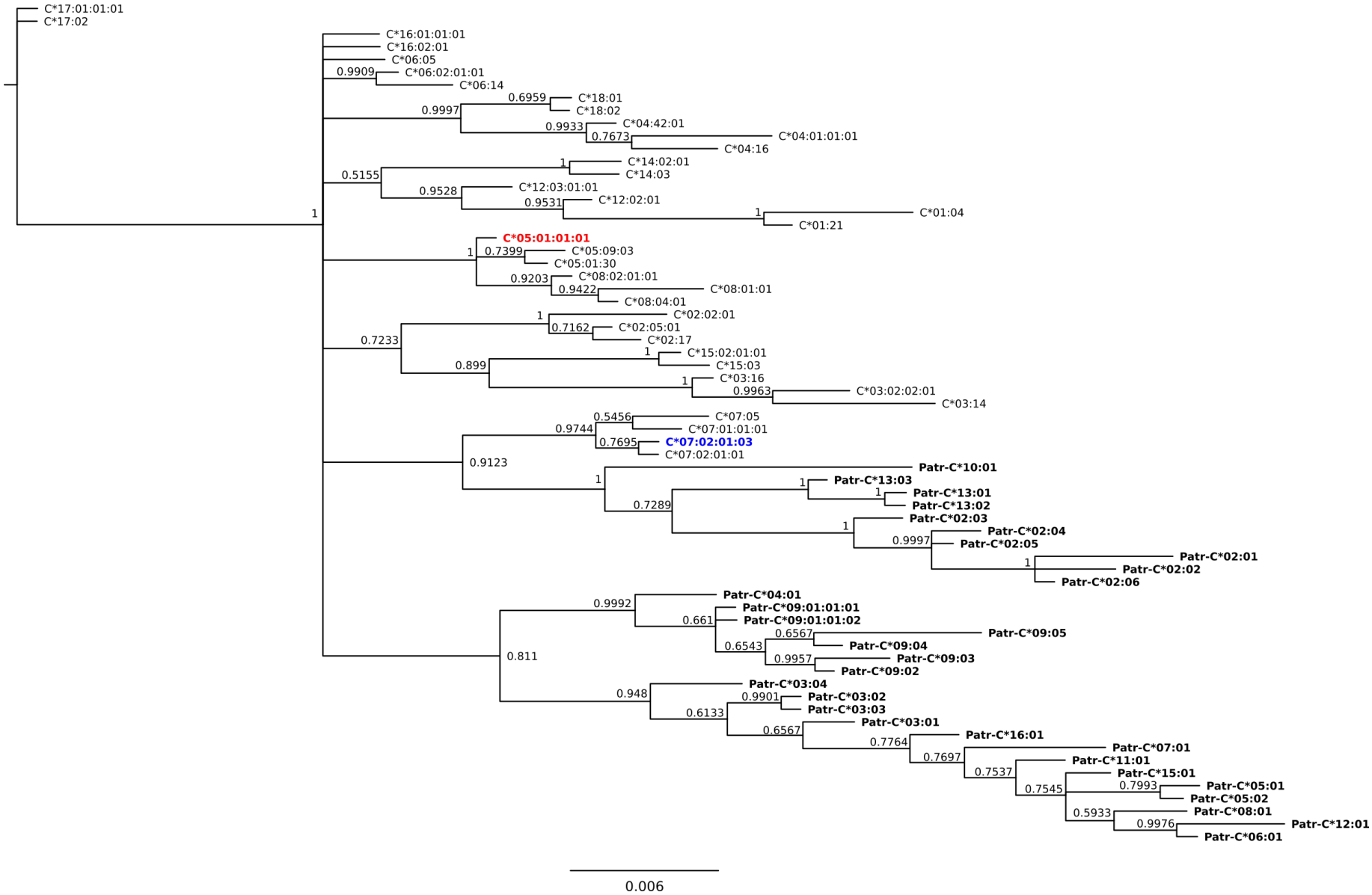

Fig. 8 - Phylogenetic analysis of human *HLA-C* and chimpanzee *MHC-C* sequences in the exons 2 and 3 region

HLA-C exon 2 and exon 3 sequences were aligned and used to infer phylogenetic relationship. Nodes are labelled with the estimated posterior for each split in the tree. The scale represents expected substitutions per site. *HLA-C*05:01:01:01* (red), *HLA-C*07:02:01:03* (blue), other *HLA-C* alleles (black) and chimpanzee *Patr-C* alleles (black bold) are shown.

Figure 9

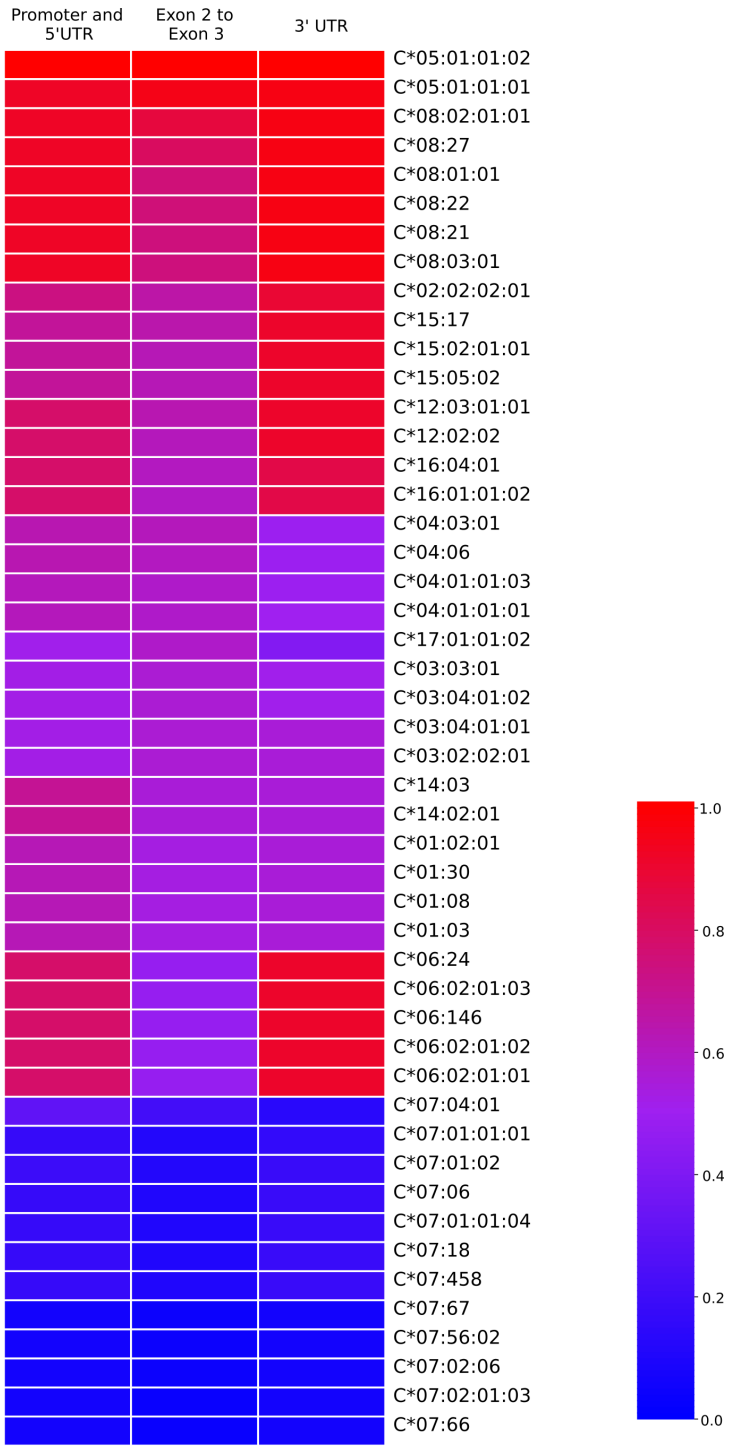

Fig. 9 - Patterns of genetic diversity in human *HLA-C* alleles at three regulatory sites

Each grid represents the similarity between a *HLA-C* allele and the *HLA-C*05:01:01:01* and *HLA-C*07:02:01:03* alleles, and it is coloured based on its similarity to *C*05*. Similarity is determined through phylogenetic analysis at the promoter/5'UTR, exon 2-3, and 3'UTR regions. The display of HLA-C subgroup alleles is based on their similarity ranking in the exon 2-3 region. Inferred trees utilised to extract these similarities are presented in Supplementary Fig. 6.

Figure 10

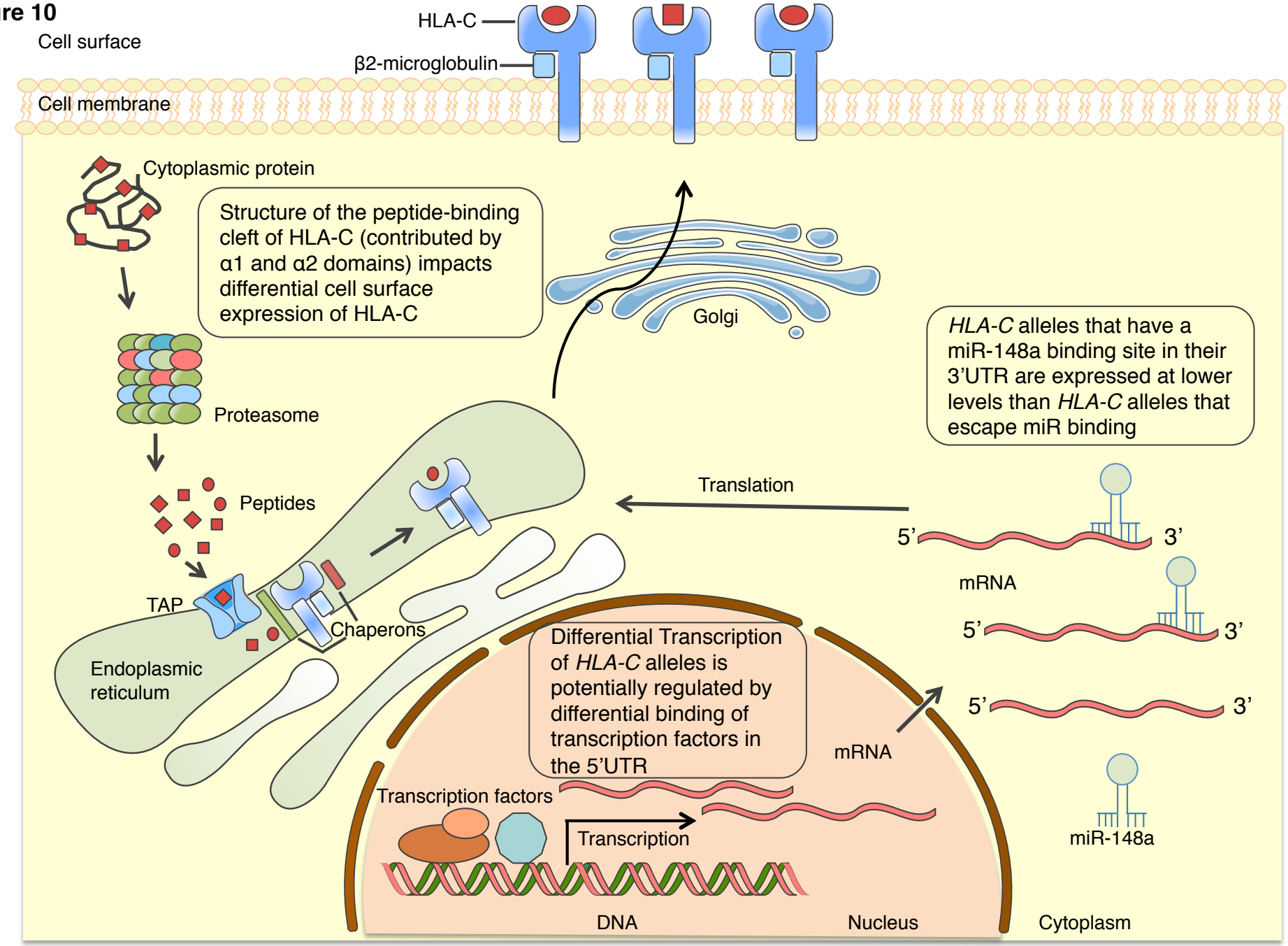

Fig. 10 - The regulatory landscape of HLA-C expression

A combination of variants in the 5'UTR, the antigen-binding cleft, and the 3'UTR, and potentially other yet unidentified factors, drive differential HLA-C expression at the cell-surface.